



Discover Generics

Cost-Effective CT & MRI Contrast Agents



WATCH VIDEO

AJNR

Reassessing the Carotid Artery Plaque "Rim Sign" on CTA: A New Analysis with Histopathologic Confirmation

J.C. Benson, V. Nardi, A.A. Madhavan, M.C. Bois, L. Saba, L. Savastano, A. Lerman and G. Lanzino

This information is current as of June 25, 2025.

AJNR Am J Neuroradiol 2022, 43 (3) 429-434

doi: <https://doi.org/10.3174/ajnr.A7443>

<http://www.ajnr.org/content/43/3/429>

Reassessing the Carotid Artery Plaque “Rim Sign” on CTA: A New Analysis with Histopathologic Confirmation

J.C. Benson, V. Nardi, A.A. Madhavan, M.C. Bois, L. Saba, L. Savastano, A. Lerman, and G. Lanzino



ABSTRACT

BACKGROUND AND PURPOSE: The CTA “rim sign” has been proposed as an imaging marker of intraplaque hemorrhage in carotid plaques. This study sought to investigate such findings using histopathologic confirmation.

MATERIALS AND METHODS: Included patients had CTA neck imaging <1 year before carotid endarterectomy. On imaging, luminal stenosis and the presence of adventitial (<2-mm peripheral) and “bulky” (≥ 2 -mm) calcifications, total plaque thickness, soft-tissue plaque thickness, calcification thickness, and the presence of ulcerations were assessed. The rim sign was defined as the presence of adventitial calcifications with internal soft-tissue plaque of ≥ 2 mm in maximum thickness. Carotid endarterectomy specimens were assessed for both the presence and the proportional makeup of lipid material, intraplaque hemorrhage, and calcification.

RESULTS: Sixty-seven patients were included. Twenty-three (34.3%) were women; the average age was 70.4 years. Thirty-eight (57.7%) plaques had a rim sign on imaging, with strong interobserver agreement ($\kappa = 0.85$). A lipid core was present in 64 (95.5%) plaques (average, 22.2% proportion of plaque composition); intraplaque hemorrhage was present in 52 (77.6%), making up, on average, 13.7% of the plaque composition. The rim sign was not associated with the presence of intraplaque hemorrhage ($P = .11$); however, it was associated with a greater proportion of intraplaque hemorrhage in a plaque ($P = .049$). The sensitivity and specificity of the rim sign for intraplaque hemorrhage were 61.5% and 60.0%, respectively.

CONCLUSIONS: The rim sign is not associated with the presence of intraplaque hemorrhage on histology. However, it is associated with a higher proportion of hemorrhage within a plaque and therefore may be a biomarker of more severe intraplaque hemorrhage, if present.

ABBREVIATIONS: CEA = carotid endarterectomy; IPH = intraplaque hemorrhage; LRNC = lipid-rich necrotic core

Atherosclerotic disease in the large vessels of the head and neck is responsible for up to 15% of ischemic strokes, and the carotid bifurcation is particularly susceptible to the formation of plaques.¹ However, it is now known whether histologic differences exist between plaques, which may make them more or less susceptible to sudden changes.² These so-called vulnerable features, eg, intraplaque hemorrhage (IPH), ulcerations, and thrombosis, are high-risk markers for ipsilateral ischemic neurologic events.^{3,4}

The criterion standard for cervical carotid plaque imaging is MRA.⁵ By means of various sequences, the presence of a lipid-rich necrotic core (LRNC) and IPH and the integrity of the fibrous cap can all be determined with a high degree of accuracy.⁶ Some

imaging biomarkers of plaque can also be identified on CTA, including the degree of stenosis, ulceration, and the presence of calcifications.⁷⁻⁹ CTA is limited, however, in its ability to distinguish between IPH and LRNC due to the overlapping attenuations between such tissues. Attempts to use the Hounsfield unit threshold to differentiate between IPH and LRNC have produced contradictory results.^{10,11} Nevertheless, the commonality with which CTA is used for stroke imaging makes it an appealing technique to optimize for carotid plaque characterization.

Some authors have used surrogate imaging biomarkers on CTA to assess the presence of IPH.¹² Both ulceration and plaque thickness, for example, have been shown to be associated with IPH.^{13,14} Others have used a combination of CTA findings and patient demographics to create a model for predicting IPH.¹² One imaging marker that gained traction as a potential indicator of IPH was the so-called “rim sign,” characterized by soft-plaque components surrounded by a ring of thin, adventitial calcification.¹⁵ If validated, this sign could serve as an essential tool for identifying symptomatic or high-risk plaques. To date, however, this sign has only been assessed in comparison with MRA; no histologic confirmation of

Received August 13, 2021; accepted after revision October 23.

From the Departments of Radiology (J.C.B., A.A.M.), Cardiovascular Medicine (V.N.), Laboratory Medicine and Pathology (M.C.B., A.L.), and Neurosurgery (L. Savastano, G.L.), Mayo Clinic, Rochester, Minnesota; and Department of Medical Sciences (L. Saba), University of Cagliari, Cagliari, Italy.

Please address correspondence to John C. Benson, MD, Department of Radiology, Mayo Clinic, 200 1st St SW, Rochester, MN 55905; e-mail: Benson.john3@mayo.edu

<http://dx.doi.org/10.3174/ajnr.A7443>

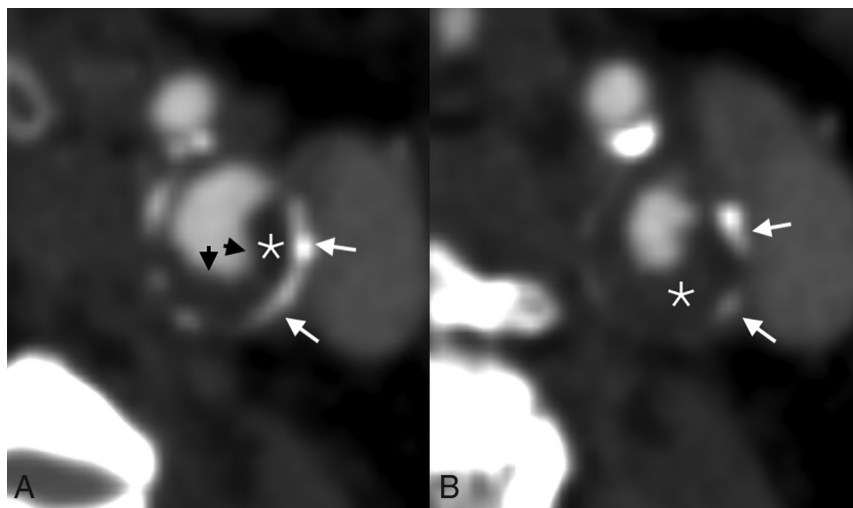


FIG 1. An example of multiple imaging biomarkers in a left carotid artery plaque. A mixed-density plaque involving the left origin (A) and proximal aspect (B) of the left ICA has adventitial calcifications (white arrows), a soft-tissue component measuring >2 mm (white star), and an ulceration (black arrows).

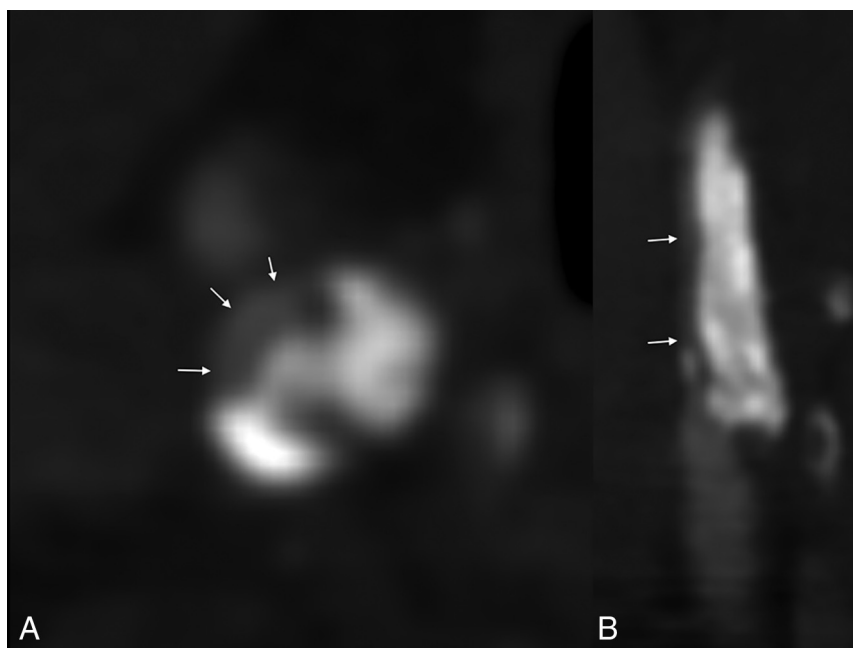


FIG 2. An example of bulky calcifications in a right carotid plaque. Axial (A) and coronal reformat (B) images demonstrate near-complete occlusion of the proximal right ICA by a large calcified plaque (arrows show residual lumen).

the rim sign exists. The current study set out to address this gap in knowledge by assessing the validity, sensitivity, and specificity of the rim sign using histopathologic comparisons.

MATERIALS AND METHODS

Patient Selection

This study was performed with approval by the local institutional review board at Mayo Clinic in Rochester, Minnesota. A

retrospective review was performed of sequential adult patients who underwent a carotid endarterectomy (CEA) between October 1, 2002, and February 1, 2020. All included patients had histologic specimens of the surgically removed tissue available for review and underwent preprocedural CTA of the cervical arterial vasculature. Patients were excluded if the time difference between CTA imaging and CEA was >1 year. A prerequisite for this study was that the images were of acceptable quality (eg, not degraded by motion artifacts), though no patients were ultimately excluded for poor-quality imaging.

CTA Protocol

This study was performed at a large institution with multiple CT scanners using imaging parameters that varied during the span of the study. Thus, the precise parameters cannot be provided for this analysis. For all examinations, however, CTA was performed of the head and neck, and the scan range was set from the cranial vertex to the carina. Intravenous access was typically achieved using an 18- or 20-ga needle in an antecubital vein. Omnipaque 350 (GE Healthcare) was administered at 4 mL/s (total 100 mL), followed by a normal saline flush at 4 mL/s (total, 35 mL). Contrast administration was initiated by a tracking voxel placed at the aortic arch. Section thickness for all examinations was 0.75 mm.

CTA Analysis

All CTA images were reviewed by a single blinded neuroradiologist (J.C.B.). Images were reviewed for the presence or absence of any calcification, adventitial (<2 -mm thickness along periphery) calcification, “bulky” calcification (≥ 2 -mm thickness, without associated adventitial calcification),

maximum luminal stenosis, maximum plaque thickness, maximum calcification thickness, maximum soft-tissue thickness, ulceration, and the rim sign (Figs 1 and 2). Ulcerations were defined as being a focal outpouching of the vessel lumen into the plaque of at least 2 mm in depth, as previously defined.¹⁶ The rim sign was defined as being adventitial calcifications with internal soft-tissue plaque of ≥ 2 mm in maximum thickness. The soft tissue needed to be between the vessel lumen and adventitial calcifications to be compatible with a rim sign. The

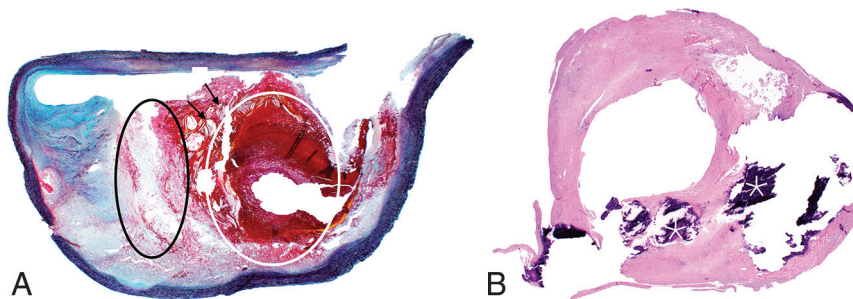


FIG 3. Histologic examples of a hemorrhagic (A) and partially calcified (B) plaque. Intraplaque-hemorrhage is represented by red tissue staining on Movat Pentachrome (white circle, A); blood products are superimposed on a lipid-rich necrotic core (represented by clear cholesterol clefts, black arrows) and white-stained tissue (black circle, A). Multiple coarse calcifications are seen in the second plaque, some of which were fragmented during the endarterectomy (asterisks) (both images are original magnification, $\times 12.5$).

Table 1: Summary of cardiovascular risk factors^a

Risk Factors	No. (%) (BMI = Mean and SD)
Ethnicity	White = 66 (98.5%) Native American = 1 (1.5%)
Tobacco use (current or prior)	45 (67.2%)
Alcohol use	31 (46.3%)
Hypertension	53 (79.1%)
Diabetes mellitus	20 (30.0%)
Average BMI (SD)	29.8 (SD = 6.3)

Note:—BMI indicates body mass index

^aNearly all patients were White, likely influenced by the demographics at the institution at which this study was completed.

definitions of adventitial and bulky calcifications and the rim sign were based on those used by Eisenmenger et al.¹⁵ Intraluminal thrombi were defined as being filling defects within the vessel lumen, sometimes called the “donut sign.”^{17,18} Maximum luminal stenosis was based on the NASCET criteria, using the diameter of the lumen at its area of greatest stenosis and a region of the uninvolved ICA distal to the carotid bulb.

A second blinded neuroradiologist performed an additional analysis of whether the rim sign was present, to perform an assessment of interrater agreement. Inconsistencies between observers were resolved with consensus agreement.

Histologic Analysis

All histologic specimens were reviewed using light microscopy by a single blinded cardiovascular pathologist (M.C.B.). On excision via CEA, all plaques were fixed in 10% buffered formalin and embedded. Sections were 5- μ m-thick. Two levels per case were reviewed, one stained with hematoxylin-eosin and one with Movat pentachrome stain (Fig 3). Analysis was performed on the level stained with the Movat stain to facilitate identification of graded tissue elements. Overall percentages of each component (if present) were estimated via light microscopy and digital analysis quantification using Aperio ImageScope (<https://www.leicabiosystems.com/us/digital-pathology/manage/aperio-imagescope/>) with manual delineation of areas of IPH and subsequent calculation.

Each specimen was assessed for the presence or absence of IPH, lipid core (LRNC), and calcification. Plaque hemorrhage was temporally classified into remote and recent as assessed by hemosiderin-laden macrophages or red blood cells and fibrin, respectively (when

applicable), though both remote and recent categories were considered to represent IPH for the purposes of statistical analysis. Lipid cores were defined as an aggregate of foamy histiocytes and/or extracellular deposits of cholesterol. Calcium was identified by its characteristic appearance on light microscopy and appeared continuous and/or plaque-like or punctate and/or multifocal. As mentioned above, semi-quantitative enumeration of the relative percentage of each component was recorded.

Statistical Analysis

Means (SDs) were calculated for all continuous variables. Categorical variables

were calculated as a proportion of the cohort. Logistic regression analyses were used for comparisons of categorical variables. Linear regression analyses were performed for comparisons among continuous variables. The κ calculation was performed to assess interobserver agreement for the presence of the rim sign. Because both adventitial calcifications and soft-tissue thickness of ≥ 2 mm were considered both confounding and deterministic variables in the assessment of the rim sign, multivariate logistic and multivariable linear regression models were also used. All calculations took place in Excel (Microsoft) and JMP statistical software (SAS Institute). Statistical significance was set to $P = .05$.

RESULTS

Patient Cohort

Of 79 patients, 12 were excluded because the time difference between CTA and CEA was >1 year. Thus, 67 patients were included in the final patient cohort. Twenty-three (34.3%) were women; the average age was 70.4 (SD, 9.1) years. A slight majority (35; 52.2%) of CEAs was completed on left-sided plaques. Cardiovascular risk factors, which have been reported elsewhere in this cohort, are detailed in Table 1.¹⁹

Imaging and Histologic Analyses

On imaging, 53 patients (79.1%) had adventitial calcifications, 11 (16.4%) had bulky calcifications, and 3 (4.5%) had no calcifications (Table 2). The average degree of maximal stenosis was 77.4% (SD, 16.5%). The overall maximum plaque thickness was 4.9 (SD, 1.5) mm. The maximum thickness of soft tissue was 4.0 (SD, 2.0) mm; the maximum thickness of calcifications was 1.9 (SD, 1.2) mm. Eleven patients (16.4%) had an ulceration, and 38 (57.7%) had a rim sign. The average time between CTA and CEA was 42.3 (SD, 64.2) days; the median time was 17 days.

On histology, a lipid core was present in 64 plaques (95.5%). When present, the relative percentage of lipid makeup of a plaque was 22.2% (SD, 19.2%). Some degree of calcification was present in 57 plaques (85.1%). When present, calcifications was an estimated 20.9% of plaque makeup (SD, 20.7%). IPH was seen in 52 (77.6%) plaques, making up an average of 13.7% (SD, 17.2%) of plaque composition when present.

Interobserver Agreement and Association Analyses

Interobserver agreement for the rim sign was strong ($\kappa = 0.85$; 95% CI, 0.72–0.96).

Associations between various imaging markers and histology are detailed in Table 3. The rim sign was not associated with the presence of IPH or LRNC ($P = .11$ and $P = .39$, respectively). However, plaques with the rim sign had a greater proportion of hemorrhage on histology (17.2% versus 8.6%, $P = .049$) as well as a greater proportion of lipid (27.3% versus 15.1%, $P = .01$). Adventitial calcifications were associated with the presence of IPH ($P = .01$), but not LRNC ($P = .046$). Plaques with adventitial calcifications had greater proportions of both IPH (16.5% versus 3.2%, $P = .009$) and LRNC (24.9% versus 11.8%, $P = .02$). Ulcerations were associated with neither the presence nor the proportion of IPH or LRNC.

Regarding the soft-tissue plaque components, the maximum thickness was significantly greater in plaques that had LRNC than in those without (4.1 [SD, 1.9] mm versus 1.4 [SD, 1.0] mm, respectively; $P = .02$). The maximum thickness was not significantly different among plaques with and without IPH (4.2 [SD, 1.9] mm versus 3.3 [SD, 2.1] mm, respectively; $P = .18$). Linear regression showed

significant associations between soft-tissue thickness and both LRNC and IPH proportions ($P = .002$ for both).

The degree of luminal stenosis was not significantly different among plaques with and without IPH (77.9% [SD, 17.3%] versus 75.6% [SD, 13.7%], respectively; $P = .59$). Plaques with LRNC, conversely, did have significantly greater stenosis (78.4% [SD, 16.2%] versus 56.7% [SD, 5.8%], respectively; $P = .006$). Linear regression showed no association between the degree of stenosis and LRNC or IPH proportions ($P = .32$ and $P = .55$, respectively).

The overall plaque thickness (calcifications and soft-tissue combined) was not significantly different among plaques containing lipid cores (4.9 [SD, 1.5] mm versus 4.0 [SD, 1.0] mm; $P = .24$) nor was it different among plaques containing IPH (5.0 [SD, 1.4] mm versus 4.4 [SD, 1.8] mm; $P = .24$).

The sensitivity and specificity of the rim sign for IPH were 61.5% and 60.0%, respectively; the positive and negative predictive values were 84.2% and 31.0%, respectively.

Multivariate Analyses

The rim sign, soft tissue of ≥ 2 mm thickness, and adventitial calcifications were all used for multivariate analyses. Of these biomarkers, only the presence of adventitial calcifications was associated with the presence of IPH ($P = .03$); none were associated with the proportion of IPH (P values ranged from .16 for adventitial calcifications to .65 for the rim sign).

By means of multivariate analyses, none of the biomarkers were associated with either the presence of LRNC (P values ranged from .11 for soft-tissue of ≥ 2 -mm thickness to .18 for adventitial calcifications) or the proportion of LRNC (P values ranged from .16 for soft-tissue of ≥ 2 -mm thickness to .71 for adventitial calcifications).

DISCUSSION

CT is a widely used second-level technique for carotid plaque imaging, but it is widely considered less capable than MR imaging for the detection of IPH. This study represents the first to assess the capability of the carotid artery plaque CT rim sign to detect IPH with histologic confirmation of plaque tissue. The results indicate that the rim sign has strong interobserver agreement but is not associated with the presence of IPH and has poor sensitivity and specificity for the detection of IPH. The rim sign is,

Table 2: Summary of imaging and histologic findings

Findings	No. (%) or Average (SD)
Imaging features	
Rim sign	39 (58.2%)
Ulceration	11 (16.4%)
Any calcifications	64 (95.5%)
Adventitial calcifications	53 (79.1%)
Bulky calcifications	11 (16.4%)
Soft tissue ≥ 2 mm	55 (82.0%)
Maximum soft-tissue thickness (mean) (mm)	4.0 (SD, 2.0)
Maximum overall plaque thickness (mean) (mm)	4.9 (SD, 1.5)
Maximum stenosis (mean) (%)	77.4 (SD, 16.5)
Histologic findings	
LRNC present	64 (95.5%)
LRNC proportion (mean)	22.2% (SD, 19.2%)
IPH present	52 (77.6%)
IPH proportion (mean)	13.7% (SD, 17.2%)
Calcification present	57 (85.1%)
Calcification proportion (mean)	20.9% (SD, 20.7%)

Table 3: Associations between various imaging markers and histology^a

	IPH (OR; 95% CI; <i>P</i> Value)	LRNC (OR; 95% CI; <i>P</i> Value)	IPH Proportion (RC; 95% CI; <i>P</i> Value)	Lipid Proportion (RC; 95% CI; <i>P</i> Value)
Rim sign	OR = 2.6 95% CI, 0.8–8.9 <i>P</i> value = .11	OR = 2.9 95% CI, 0.3–33.9 <i>P</i> value = .39	RC = 4.2 95% CI, 0.02–8.3 <i>P</i> value = .049 ^b	RC = 6.1 95% CI, 1.5–10.6 <i>P</i> value = .01 ^b
Adventitial calcifications	OR = 5.6 95% CI, 1.6–21.2 <i>P</i> value = .01 ^b	OR = 6.7 95% CI, 0.8–195.7 <i>P</i> value = .08	RC = 6.6 95% CI, 1.7–11.6 <i>P</i> value = .009 ^b	RC = 6.6 95% CI, 1.0–12.1 <i>P</i> value = .02
Ulceration	OR = 1.4 95% CI, 0.3–7.1 <i>P</i> value = .72	<i>P</i> value = .29 ^c	RC = 1.4 95% CI, –4.3–7.1 <i>P</i> value = .6	RC = 5.6 95% CI, –0.6–11.9 <i>P</i> value = .07

Note:—RC indicates regression coefficient.

^a Univariate analyses between imaging features and IPH and LRNC were calculated with logistic regression analyses with odds ratios reported; imaging features and proportions of both IPH and LRNC were calculated with linear regression analyses with regression coefficients reported.

^b Statistically significant.

^c Odds ratio could not be calculated for ulceration and LRNC due to relatively sparse data spreads.

however, associated with a greater proportion of IPH in terms of plaque composition, suggesting that it may be associated with more substantial plaque hemorrhage.

The rim sign was originally described by Eisenmenger et al,¹⁵ in 2016, using IPH detection on MRA as the criterion standard. In that study, the authors assessed 188 plaques that had undergone CTA and MRA of the carotid arteries within 1 month. The authors found numerous markers on CTA to be more common among the plaques with IPH, including a greater degree of stenosis, maximum plaque thickness, maximum soft-tissue plaque thickness, maximum hard-plaque thickness, and ulceration. Using a multivariable Poisson regression, the authors found that the model that was best predictive of IPH included the presence of a rim sign (prevalence ratio = 11.9) and maximum soft-tissue plaque thickness (prevalence ratio = 1.2). The patient cohort in the current study had more substantial disease burden of carotid atherosclerotic plaque, likely related to differences in the inclusion criteria. Most patients in the current study had IPH, whereas this was noted in a minority of patients in the Eisenmenger et al cohort.

Baradaran et al²⁰ built on such findings by assessing CTA biomarkers as predictors of ipsilateral stroke. In their study, the authors found that multiple plaque characteristics were more common in the carotid artery ipsilateral to the patient's stroke, including ulceration, increased plaque thickness (total, soft, and calcified), and the rim sign. Like Eisenmenger et al,¹⁵ the authors performed a multivariable regression analysis with elimination of potential confounders. The final model proposed by Eisenmenger et al was composed of the maximum soft-plaque thickness and the rim sign, like findings in the preceding study, as well as intraluminal thrombus.

One possible explanation between the differences in the results of the current study and those of Eisenmenger et al¹⁵ is that relatively small amounts of IPH are not detected on MRA but were visible on histology. The current study did demonstrate that plaques with the rim sign had significantly greater proportions of hemorrhage. Because Eisenmenger et al used MRA as the criterion standard, it is, therefore, possible that plaques with tiny amounts of hemorrhage did not meet the threshold to be detected on MR imaging.

Nevertheless, a convincing explanatory pathomechanism for the rim sign is yet to be established. Both Eisenmenger et al¹⁵ and Baradaran et al²⁰ hypothesized that its association with IPH suggests that adventitial calcifications may represent sequelae of neovascular proliferation and inflammation.¹⁵ The current study found that adventitial calcifications were associated with IPH, even on multivariate analyses, possibly offering evidence for this hypothesis. However, it also seems plausible that the presence of adventitial calcifications simply serves as a proxy for the absence of their bulkier counterparts. After all, it is known that bulky calcifications are a marker of relatively stable plaques.²¹ Gupta et al²² showed that for each 1-mm increase in calcification diameter, the odds of symptomatology decreased by 80%. Adventitial calcifications, therefore, may be seen in plaques that are more prone to develop large soft-tissue components that can hemorrhage, while bulky calcifications signify a plaque that has taken a more stable, quiescent route of growth. The presence of soft tissue of

≥2 mm, similarly, may simply serve as a marker for relatively large soft plaques that are prone to develop IPH. This is in line with a prior study which showed larger atherosclerotic lesions are associated with higher-grade plaques on MR imaging.²³ It may therefore be best to consider the rim sign as a surrogate for possible IPH. MRA remains the criterion standard for carotid plaque characterization.²⁴

This study shares the limitations of all retrospective analyses. In addition, the study did not set out to assess the findings in the setting of symptomatology. The clinical effect of any observed IPH is, therefore, uncertain. Next, the studied cohort had relatively large plaques, with an average degree of stenosis of 77.4%. Thus, it is uncertain whether the observed effects would remain true in smaller, less stenotic plaques. In addition, the time gap between CTA and CEA represents a potential confounding variable. It is possible that changes occurred in the composition of carotid plaques in the interim between imaging and surgery, though the median time interval between imaging and surgery (17 days) was relatively short. Finally, the cohort studied represents a specific population, and it is uncertain whether the observed results can be generalized elsewhere.

CONCLUSIONS

By means of histopathology as the criterion standard, the carotid artery plaque rim sign is not associated with the presence of IPH and has poor sensitivity and specificity for predicting IPH. However, plaques with the rim sign did have a greater amount of hemorrhage as a proportion of plaque composition, suggesting that the sign may serve as a biomarker for higher degrees of plaque hemorrhage, if present.

Disclosure forms provided by the authors are available with the full text and PDF of this article at www.ajnr.org.

REFERENCES

1. Cole JW. Large artery atherosclerotic occlusive disease. *Continuum (Minneapolis)* 2017;23:133–57 [CrossRef Medline](#)
2. Benson JC, Cheek H, Aubry MC, et al. Cervical carotid plaque MRI: review of atherosclerosis imaging features and their histologic underpinnings. *Clin Neuroradiol* 2021;31:295–306 [CrossRef Medline](#)
3. Brinjikji W, Huston J, Rabinstein AA, et al. Contemporary carotid imaging: from degree of stenosis to plaque vulnerability. *J Neurosurg* 2016;124:27–42 [CrossRef Medline](#)
4. Alkhouli M, Holmes D, Klaas JP, et al. Carotid intraplaque hemorrhage: an underappreciated cause of unexplained recurrent stroke. *JACC Cardiovasc Interv* 2021;14:1950–52 [CrossRef Medline](#)
5. Fitzpatrick LA, Berkovitz N, Dos Santos MP, et al. Vulnerable carotid plaque imaging and histopathology without a dedicated MRI receiver coil. *Neuroradiol J* 2017;30:120–28 [CrossRef Medline](#)
6. Singh N, Moody AR, Roifman I, et al. Advanced MRI for carotid plaque imaging. *Int J Cardiovasc Imaging* 2016;32:83–89 [CrossRef Medline](#)
7. Murgia A, Erta M, Suri JS, et al. CT imaging features of carotid artery plaque vulnerability. *Ann Transl Med* 2020;8:1261 [CrossRef Medline](#)
8. Baradaran H, Foster T, Harrie P, et al. Carotid artery plaque characteristics: current reporting practices on CT angiography. *Neuroradiology* 2021;63:1013–18 [CrossRef Medline](#)
9. Saba L, Brinjikji W, Spence JD, et al. Roadmap consensus on carotid artery plaque imaging and impact on therapy strategies and

- guidelines: an international, multispecialty, expert review and position statement. *AJNR Am J Neuroradiol* 2021;42:1566–75 [CrossRef](#) [Medline](#)
10. Saba L, Francone M, Bassareo PP, et al. **CT attenuation analysis of carotid intraplaque hemorrhage.** *AJNR Am J Neuroradiol* 2018;39:131–37 [CrossRef](#) [Medline](#)
 11. Wintermark M, Jawadi SS, Rapp JH, et al. **High-resolution CT imaging of carotid artery atherosclerotic plaques.** *AJNR Am J Neuroradiol* 2008;29:875–82 [CrossRef](#) [Medline](#)
 12. McLaughlin MS, Hinckley PJ, Treiman SM, et al. **Optimal prediction of carotid intraplaque hemorrhage using clinical and lumen imaging markers.** *AJNR Am J Neuroradiol* 2015;36:2360–66 [CrossRef](#) [Medline](#)
 13. U-King-Im JM, Fox AJ, Aviv RI, et al. **Characterization of carotid plaque hemorrhage.** *Stroke* 2010;41:1623–29 [CrossRef](#) [Medline](#)
 14. Gupta A, Baradaran H, Mtui EE, et al. **Detection of symptomatic carotid plaque using source data from MR and CT angiography: a correlative study.** *Cerebrovasc Dis* 2015;39:151–61 [CrossRef](#) [Medline](#)
 15. Eisenmenger LB, Aldred BW, Kim SE, et al. **Prediction of carotid intraplaque hemorrhage using adventitial calcification and plaque thickness on CTA.** *AJNR Am J Neuroradiol* 2016;37:1496–1503 [CrossRef](#) [Medline](#)
 16. Yuan J, Usman A, Das T, et al. **Imaging carotid atherosclerosis plaque ulceration: comparison of advanced imaging modalities and recent developments.** *AJNR Am J Neuroradiol* 2017;38:664–71 [CrossRef](#) [Medline](#)
 17. Menon BK, Singh J, Al-Khataami A, et al; for the Calgary CTA Study Group. **The donut sign on CT angiography: an indicator of reversible intraluminal carotid thrombus?** *Neuroradiology* 2010;52:1055–56 [CrossRef](#) [Medline](#)
 18. Singh R-J, Chakraborty D, Dey S, et al. **Intraluminal thrombi in the cervico-cephalic arteries.** *Stroke* 2019;50:357–64 [CrossRef](#) [Medline](#)
 19. Benson JC, Lanzino G, Nardi V, et al. **Semiautomated carotid artery plaque composition: are intraplaque CT imaging features associated with cardiovascular risk factors?** *Neuroradiology* 2021;63:1617–26 [CrossRef](#) [Medline](#)
 20. Baradaran H, Eisenmenger LB, Hinckley PJ, et al. **Optimal carotid plaque features on computed tomography angiography associated with ischemic stroke.** *J Am Heart Assoc* 2021;10:e019462 [CrossRef](#) [Medline](#)
 21. Shaalan WE, Cheng H, Gewertz B, et al. **Degree of carotid plaque calcification in relation to symptomatic outcome and plaque inflammation.** *J Vasc Surg* 2004;40:262–69 [CrossRef](#) [Medline](#)
 22. Gupta A, Mtui EE, Baradaran H, et al. **CT angiographic features of symptom-producing plaque in moderate-grade carotid artery stenosis.** *AJNR Am J Neuroradiol* 2015;36:349–54 [CrossRef](#) [Medline](#)
 23. Trelles M, Eberhardt KM, Buchholz M, et al. **CTA for screening of complicated atherosclerotic carotid plaque: American Heart Association type VI lesions as defined by MRI.** *AJNR Am J Neuroradiol* 2013;34:2331–37 [CrossRef](#) [Medline](#)
 24. Saba L, Yuan C, Hatsukami TS, et al; Vessel Wall Imaging Study Group of the American Society of Neuroradiology. **Carotid Artery Wall Imaging: Perspective and Guidelines from the ASNR Vessel Wall Imaging Study Group and Expert Consensus Recommendations of the American Society of Neuroradiology.** *AJNR Am J Neuroradiol* 2018;39:E9–E31 [CrossRef](#) [Medline](#)